

R. V. Puzik,
orcid.org/0000-0002-9745-058X,
V. Y. Kondus*,
orcid.org/0000-0003-3116-7455,
I. V. Pavlenko,
orcid.org/0000-0002-6136-1040,
S. S. Antonenko,
orcid.org/0009-0002-7490-2691

Sumy State University, Sumy, Ukraine
* Corresponding author e-mail: v.kondus@pgm.sumdu.edu.ua

THE INFLUENCE OF THE IMPELLER DESIGN FEATURES ON THE COMBINED OPERATING PROCESS OF THE TORQUE-FLOW PUMP

Purpose. Evaluation of the effect of changing the width of the impeller blades on the characteristics of a torque-flow pump. Searching for the optimal blade extension into the free chamber of the pump. A torque-flow pump of the “Turo” type SVN 500/32 was chosen as the subject of the research work.

Methodology. A number of numerical experiments were conducted to determine the flow structure in the flowing part of a torque-flow pump. The width of the impeller blade was chosen as a variable. Numerical experiments were carried out using the ANSYS CFX software package. The integral parameters of the researched pump were determined in order to build the integral characteristics.

Findings. The structure of the general flow and toroidal vortex was studied and analyzed in the torque-flow pump. A flow model was built in a torque-flow pumps with basic and modernized design. A relationship between the parameters of the pump and the change in the impeller blade width was found. The width of the impeller blade was changed in the range from $\Delta_{\min} = -20$ to $\Delta_{\max} = +100$ mm.

Originality. The paper researched the effect of additional hydraulic losses caused by the mismatch between the center of the toroidal vortex and the edges of the impeller blades on the integral characteristics of the torque-flow pump.

Practical value. A significant increase in the operating parameters of the “Turo” type torque-flow pump was achieved with the help of modernization of the impeller design. This allows expanding the range of the pump’s operation. At the same time, it is not required to replace such expensive elements as the pump casing.

Keywords: *torque-flow pump, Ansys CFX, toroidal vortex, vortex operating process, bladed operating process*

Introduction. Currently, transportation of mineral raw materials and products of their processing is one of the most energy-consuming industries [1, 2]. Thus, modernization and improvement of the efficiency of operated equipment of hydraulic pipeline transport is one of the priority tasks of industry [3].

Centrifugal pumps have become widely used for pumping water or other pure liquids. Nevertheless, there is often a need to pump liquid containing solid or gaseous inclusions, suspensions of high viscosity, mixtures with sand, fibrous inclusions and other contaminated liquids.

One of the ways to resolve this problem is using torque-flow pumps, which are characterized by a semi-open impeller installed in the rear part of the pump casing. According to it, an enlarged free camera appears in front of the impeller. This design feature allows torque-flow pumps to transport liquids containing significant concentrations of solid or gaseous inclusions, with a reduced probability of clogging of their flowing parts. Thus, the fields of application of torque-flow pumps cover a wide range of industry from wastewater transportation to the food industry. However, the hydraulic efficiency of torque-flow pumps is lower, compared to conventional centrifugal pumps (pump efficiency does not exceed $\eta = 0.63$) [4, 5].

The effect of changing the width of the impeller blade on the characteristics and structure of the flow in the torque-flow pump flowing part was researched in papers [6, 7] in order to increase its efficiency and head. The solution to this issue is urgent, since the efficiency of torque-flow pumps of the “Turo” type decreases sharply in the areas of low ($n_s \leq 60$) and high specific speed ($n_s \geq 140$) [8, 9].

Literary review. The issue of modernizing and increasing the efficiency of hydraulic pipeline transport equipment is one of the priority tasks of the modern industrial sphere. Thus, there is a need of modernizing and improving the design of torque-flow pumps.

Cutting the impeller of a torque-flow pump is one of the effective methods for changing the parameters of the pump,

because it affects not only on the impeller characteristics itself, but also leads to a change in the free chamber size (the gap between the rotor blades and the casing wall). In relation to torque-flow pumps of the “Seka” type the method can be used for decreasing impeller blade width by means of its cutting. The maximum cutting of the blade should not exceed 10 % [10, 11], because it can be accompanied by a constant decrease in the pump head and efficiency.

Cutting every other blade of the impeller, i.e. the transition to an analogue of a two-tiered impeller in a centrifugal pumps, leads to increasing pump head and efficiency and reaches a maximum when the length of the short blades is approximately half of the length of long blades. In this case, the pump efficiency can increase up to 2–3 % [12].

Another method for reaching the demanded parameters of torque-flow pumps is extending of the impeller into the free chamber. This method can be used for torque-flow pumps of the “Turo” type. At the same time, the maximum increase in the head ($\bar{H} = 1.15$) and efficiency ($\eta = 0.535$) is observed when the impeller is fully extended to the free chamber. According to this way, the pump becomes “Seka” design scheme analog. When the impeller is extended to the free chamber, the efficiency increases, which can be justified by increasing of the intensity of the flow and decreasing of hydraulic losses during the rotation of the liquid in the pump free chamber. At the same time, the best-efficiency point (BEP) mode of the pump operation shifts towards higher flow rates [12].

Modernization of torque-flow pumps by replacing the impellers with straight blades for similar ones with profiled blades is described in research studies [4, 5]. This method allows increasing the energy efficiency of the pump up to 4–5 % and at the same time does not require replacement of such expensive elements as the pump casing. Also, the impeller with profiled blades has significantly better integral characteristics while pumping liquids with inclusions [8].

Designing the impeller with winglets allows increasing the head and efficiency of torque-flow pumps [13, 14]. However, it should be noted that in these papers, experiments were carried out during pumping pure water, while these modifications may

lead to deterioration of the pump's ability of contaminated liquids transporting [15, 16].

Theoretical research. The entire operating process of a torque-flow pump can be conditionally divided into several components [8]. After the liquid enters through the suction nozzle, the flow is divided into two main parts. One of its components forms a flowing stream and is directed into the pressure nozzle. The second component, having passed through the impeller interblade channels, continues to circulate in the flowing part and forms a toroidal vortex (Fig. 1). This vortex, so-called "liquid blade", is responsible for transferring the energy to the flowing stream, which does not directly interact with the blades of the impeller.

It should be noted that the maximum theoretically achievable efficiency of the vortex operating process is equal to 0.5, and the maximum theoretically achievable efficiency of the blade operating process is 1.0, which explains the relatively low overall efficiency of torque-flow pumps.

Torque-flow pumps of "Turo" type with a high specific speed n_s are characterized by a design with an impeller blade width smaller than the width of the free chamber (orange line in Fig. 1).

At the same time, the center of the toroidal vortex is located in the free chamber. The asymmetry of the mutual location of the blades and the vortex leads to the deformation of it, since in the area between the edge of the blade and the center of the toroidal vortex, there is an interaction of the liquid and the flow. It leads to changing of a toroidal vortex shape. This is the reason for the appearance of additional hydraulic losses in the pump flowing part [17, 18].

Impeller overall diameter cutting (red line in Fig. 1) leads to additional increasing of the vortex operating process role and decreasing of the blade operating process role. The location of the blades edges far from the center of the toroidal vortex is the cause of its significant deformation and, as a result, decrease in the overall efficiency of the torque-flow pump [7, 8].

The location of the center of the toroidal vortex directly on the edge of the blades (the blue line in Fig. 1, which corresponds to $\Delta b_2 \approx +30$ mm – the design parameters of the pump under research will be described in more details in section 3) allows avoiding deformation of the vortex at the impeller outlet. At the same time, the circular velocity of the transverse vortex increases, and the cyclicity of the vortex also increases. In this way, the energy transfer of the liquid flow is optimized, which leads to increasing of the modernized pump head and efficiency.

With a slight further expansion of the blade to a value b_2 greater than the width of the pump free chamber (green line in Fig. 1), which corresponds to $\Delta b_2 \approx +50$ mm, the center of the toroidal vortex is located in the area of the impeller interblade channels, which is typical for torque-flow pumps with a low specific speed n_s . Thus, two simultaneous processes are observed:

- firstly, the share of the blade operating process increases and the part of the liquid can directly pass from the impeller to the discharge nozzle under the action of centrifugal forces. At

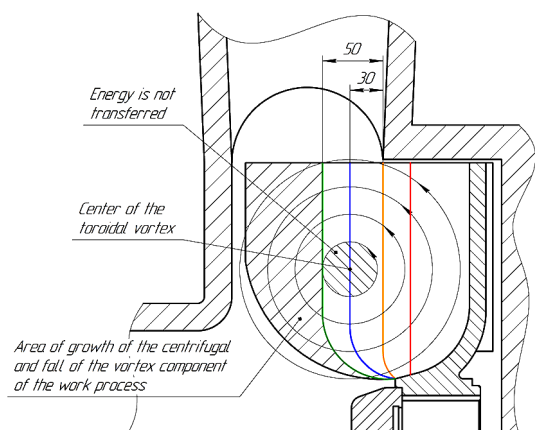


Fig. 1. Diagram of a toroidal vortex in a torque-flow pump

the same time, the head, that is the specific energy of the liquid, and the efficiency of the torque-flow pump increase;

- secondly, the deformation of the toroidal vortex, the reverse of the one described above, appears. This is due to the fact, that in the area between the center of the toroidal vortex and the blades edges (the area between the blue and green lines in Fig. 1) the liquid tries to move from the periphery to the axis of the pump. However, the action of centrifugal forces is directed liquid in the opposite direction, from the center to the periphery. This is the reason for the additional hydraulic losses' appearance.

In the area near the toroidal vortex center, where there is an extremely complex movement with intensive mixing of liquid layers, energy is practically not supplied. Therefore, when the blades edges slightly protrude beyond the center of the toroidal vortex, negative phenomena plays only a minor role.

With an additional increase in the blade width (b_2), the aforementioned phenomena increase. The part of the blade operating process becomes predominant. Thus, the torque-flow pump actually turns into a centrifugal pump with a semi-open impeller. This type pumps have significantly higher efficiency and head compared to torque-flow pumps [19]. Nevertheless, the area from the center of the toroidal vortex to the edges of the impeller blades (shaded area in Fig. 1) is the area of significant hydraulic losses since the direction of fluid movement in the toroidal vortex and the direction of action of centrifugal forces are opposite.

Used Calculated Methods. Model of the researched pump.

Parameters of the pump model. The torque-flow pump SVN 500/32 was chosen as the subject of the research (Fig. 2). The flow rate at the BEP mode is 500 m³/h, the estimated head is 32 m of water column, shaft rotation frequency is 1500 rpm. The geometric parameters of the basic model of this pump, obtained using engineering calculations, are listed in the Table.

Modernization of the flowing part of the pump. Modernization of the pump flowing part took place due to changing the impeller blades width b_2 (Fig. 3). The research was conducted in the range from $\Delta_{\min} = -20$ to $\Delta_{\max} = +100$ mm.

At the same time, the other geometric parameters remain absolutely unchanged. This makes it possible to obtain the dependence of the integral characteristics changing of the torque-flow pump exclusively on the impeller blade width b_2 .

Preparation for conducting numerical research. In order to conduct numerical research, a model of the flowing part of the researched pump was built using SolidWorks software. It, in turn, was divided into two parts: stator (pump casing) and rotor (impeller).

The construction of the calculation grid was carried out using the ICFM CFD package. That allowed obtaining an unstructured calculation grid. The entire area was firstly divided into cells in the form of a tetrahedron, followed by quality control and smoothing. Then the wall layers of prismatic cells were built (Fig. 4).

The calculation grid parameters are the next: the number of elements of stator is 1 million cells and the number of elements of rotor is 2.2 million cells. As a result of conducting a test to avoid the influence of grid density on calculation results, it was

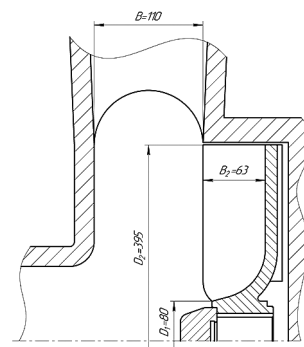


Fig. 2. Design of the flowing part of the researched pump

Table

Geometrical parameters of the flowing part of the researched pump

The relative outer diameter of the impeller	The relative diameter of the inlet of the impeller	The relative width of the impeller blade	The number of blades
\bar{D} , mm	$\bar{D}_1 = D_1/D_2$	$\bar{b}_2 = b_2/D_2$	N
1	0.2	0.16	6
The relative width of the free chamber	The relative diameter of the suction nozzle	The relative diameter of the discharge nozzle	Specific speed
$\bar{B} = B/D_2$	$\bar{D}_{suc} = D_{suc}/D_2$	$\bar{D}_{dis} = D_{dis}/D_2$	n_s
0.28	0.38	0.32	155

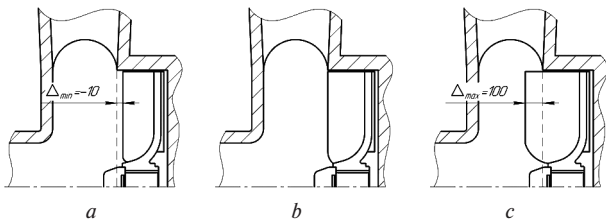


Fig. 3. Scheme of the flowing part of the pump:

a – with a reduced width of the impeller blade; b – with a standard width of the impeller blade width; c – with an increased width of the impeller blade

determined that further thickening of the calculation grid has almost no effect on the obtained experimental results.

The calculation model was created in the CFX-Pre package. The standard $k-\epsilon$ model of turbulence was used to complete the Reynolds equations, as it has proven itself well in the calculation of internal flows, has a relatively low resource intensity, and is characterized by high accuracy of results in the research on torque-flow pumps [20].

The mass flow rate was set as a boundary condition at the inlet of the calculation area. The inlet boundary is placed at a sufficient distance from the edge of the blade.

Static pressure was set as a boundary condition at the outlet of the calculation area, since in the future, all studies and comparisons were carried out using relative values.

Research plan. The aim of the research is to identify the influence of the blade width of the impeller on the characteristics of the torque-flow pump. Thus, it was decided to conduct a series of researches with a gradual change of the impeller blade width in the range from cutting the blade by 20 mm to the corresponding extension by 100 mm. In order to build integral characteristics, research on the torque-flow pump operation was carried out in the flow rate range from $Q_{min} = 0.7Q_{nom}$ to $Q_{max} = 1.2Q_{nom}$.

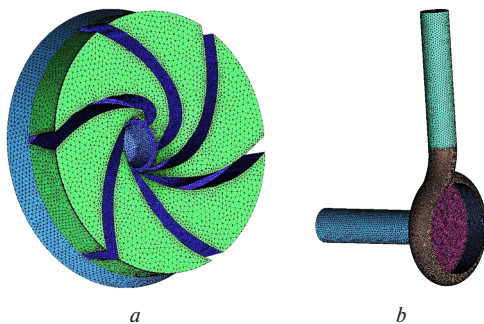


Fig. 4. Topology of the calculation grid of the rotor (a) and the stator (b) elements

The numerical research was carried out using the ANSYS CFX software package.

Analysis of the obtained results was carried out in graphic and numerical forms. The graphic form consists in the study of the flow inside the flowing part, in particular, the analysis of the fluid flow line, and the process of their evolution depending on the shape of the impeller. The numerical form allows finding the main necessary numerical parameters (for example, head, efficiency, etc.).

For the graphical analysis of the results, 4 planes perpendicular to the pump axis (Fig. 5), where there were liquid flow lines, were chosen:

Plane I – at a distance of 5 mm from the front wall of the case.

Plane II – in the center of the free chamber.

Plane III – at a distance of 5 mm from the cylindrical bore of the pump casing.

Plane IV – at a distance of 5 mm from the impeller disk.

Analysis of the results of the numerical research. Based on the obtained results of the numerical research, the dependencies of the efficiency and head of the torque-flow pump were constructed at different values of the blade width of the impeller (Fig. 6).

Let us analyze the most characteristic areas.

Impeller of the basic construction. The process of transferring energy from the impeller to the liquid inside the torque-flow pump can be conditionally divided into two stages. Firstly, the fluid flows from the suction nozzle to the impeller, where energy is transferred from the blades to the toroidal vortex. A certain part of the liquid directly flows from the inter-blade channels of the impeller to the pressure nozzle of the pump. At the second stage, the energy is transferred from the toroidal vortex to the flowing stream. In this case, the toroidal vortex acts as a so-called “liquid blade”, which, as a result of the force interaction with the flowing stream, transfers to it some moment of the motion amount (Fig. 7).

In the researched pump of the basic construction, the impeller blade width b_2 is smaller than the width of the free chamber B . This feature is typical for torque-flow pumps of the “Turo” type with a high specific speed n_s . At the same time, the share of the vortex operating process prevails over the blade operating process, which is one of the reasons for the relatively low efficiency of the torque-flow pump (the maximum theoretically achievable efficiency of the vortex operating process is approximately equal to 0.5, and that of the bladed is 1).

Thus, at the OPT mode, we get:

Head: $H_{opt}^0 = 32.3$ m;

Efficiency: $\eta_{opt}^0 = 0.34$.

Another reason for decreasing the efficiency is the deformation of the toroidal vortex caused by the asymmetry of its

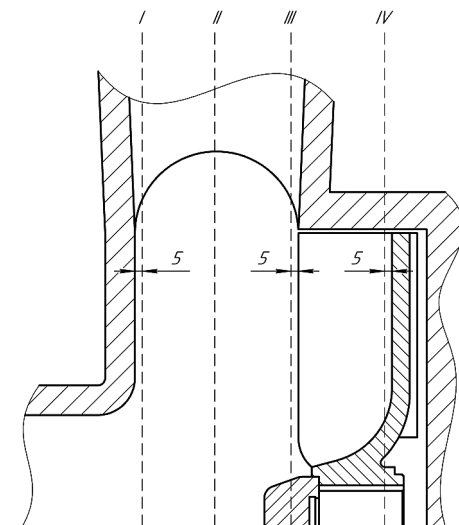


Fig. 5. Control plane selection plan

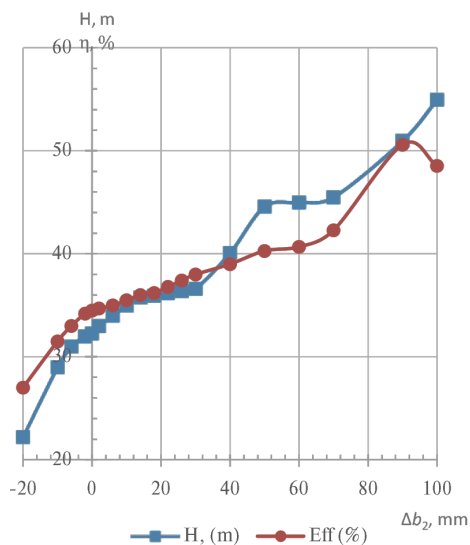


Fig. 6. Dependence of pressure and efficiency on the impeller blade width

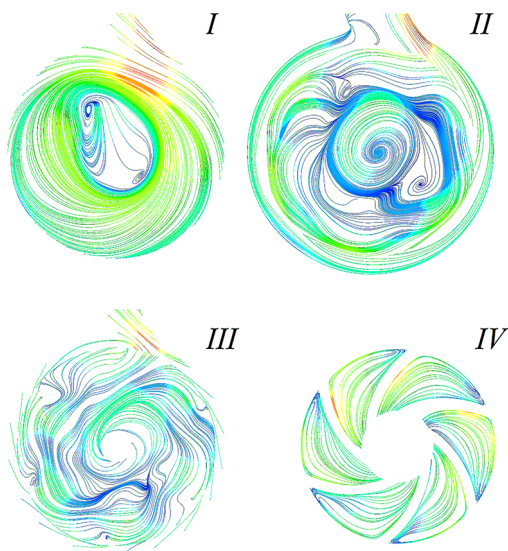


Fig. 7. Distribution of flow lines in the pump of the basic design $\Delta b_2 = 0 \text{ mm}$

location relative to the blade of the impeller. Due to the fact, that the center of the vortex is in the free chamber, there is an uneven force interaction with the blades, which leads to the appearance of additional hydraulic energy losses.

Modified impeller $\Delta b_2 = -20 \text{ mm}$. While cutting the impeller along the front end of the blades, decreasing efficiency and head is observed.

At the OPT mode, we get:

$$\text{Head: } H_{opt}^{-20} = 22.2 \text{ m;}$$

$$\text{Efficiency: } \eta_{opt}^{-20} = 0.27.$$

This is due to the fact that when the blade width is reduced, the force interaction with the fluid flow and, accordingly, the amount of energy that can be transferred from the impeller to the flow is weakened.

Since the entire impeller is located in the depth of the cylindrical bore of the pump casing, the blade operating process becomes less pronounced. As a result, a vortex operating process becomes dominant. According to this, the “liquid vane” serves as the only source of energy for the flow. Also, the number of cycles of rotation of the liquid with a toroidal vortex before it reaches the pressure nozzle increases.

Nevertheless, the direction of the vortex movement of the liquid almost completely coincides with the direction of centrifugal forces action, which positively affects the development of the vortex operating process in the pump flowing part. The toroidal vortex itself moves to the cylindrical bore of the pump casing (Fig. 8).

An increase in the intensity of the vortex motion in the flowing part leads to a weakening of the flow and, as a result, the BEP mode shifts towards smaller flow rates.

Modified impeller $\Delta b_2 = +30 \text{ mm}$. With increasing the impeller blade width in the range $\Delta b_2 = 0 \text{--} +30 \text{ mm}$, a smooth increasing of the head and efficiency of the torque-flow pump is observed.

Thus, with $\Delta b_2 = +30 \text{ mm}$, we get:

$$\text{Head: } H_{opt}^{+30} = 36.6 \text{ m;}$$

$$\text{Efficiency: } \eta_{opt}^{+30} = 0.38.$$

The main reasons for this growth are more efficient energy transfer to the “liquid blade”. The center of the toroidal vortex is located directly on the edge of the impeller blade, which ensures the minimization of hydraulic energy losses due to the asymmetric location of this vortex relative to the blade and eliminates its deformation (Fig. 9).

The partial location of the impeller in the free chamber of the pump increases the role of the blade operating process. Since the centrifugal forces are now strong enough to move the flowing stream directly to the discharge nozzle, it leads to flow rate increasing and decreasing of the number of liquid rotation cycles in the pump free chamber.

Modified impeller $\Delta b_2 = +50 \text{ mm}$. While the width of the impeller blade is further increased (Fig. 10) in the range $\Delta b_2 = +30 \text{--} +50 \text{ mm}$, a rapid increasing of the head value is observed:

$$\text{Head: } H_{opt}^{+50} = 44.6 \text{ m;}$$

$$\text{Efficiency: } \eta_{opt}^{+50} = 0.40.$$

The main reason is increasing of the share of the blade operating process and, accordingly, decreasing of the share of the vortex operating process in the overall operating process of the torque-flow pump.

This process is accompanied by the displacement of the center of the toroidal vortex in the interblade channels of the impeller, as shown in Fig. 1. As a result, some additional hydraulic losses appear. This construction is similar to the case of a torque-flow pump with a low specific speed n_s .

Modified impeller $\Delta b_2 = +70 \text{ mm}$. In the range $\Delta b_2 = +50 \text{--} +70 \text{ mm}$, the head and efficiency values remain practically unchanged:

$$\text{Head: } H_{opt}^{+50-+70} = 45 \text{ m;}$$

$$\text{Efficiency: } \eta_{opt}^{+50-+70} = 0.41.$$

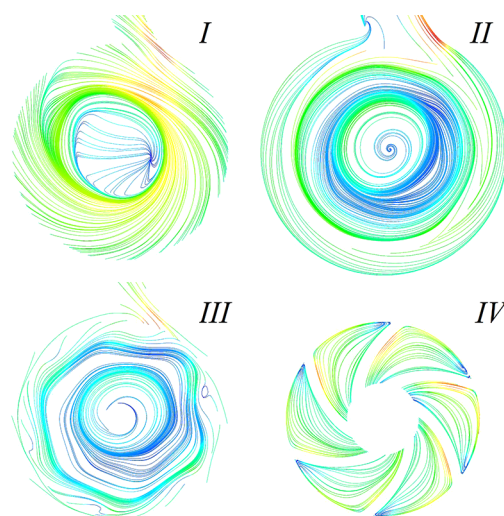


Fig. 8. Distribution of flow lines in a pump of a modified construction $\Delta b_2 = -20 \text{ mm}$

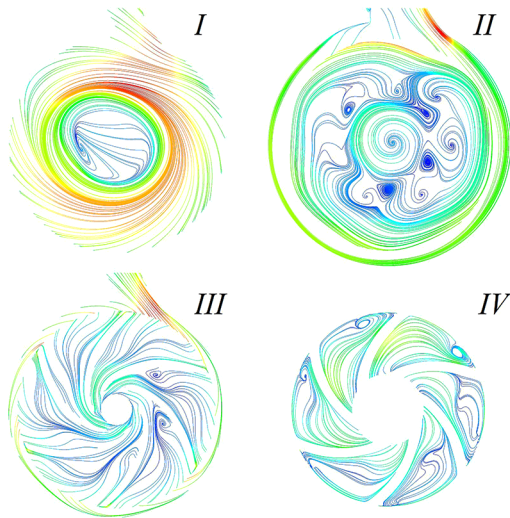


Fig. 9. Distribution of flow lines in a pump of a modified construction $\Delta b_2 = +30$ mm

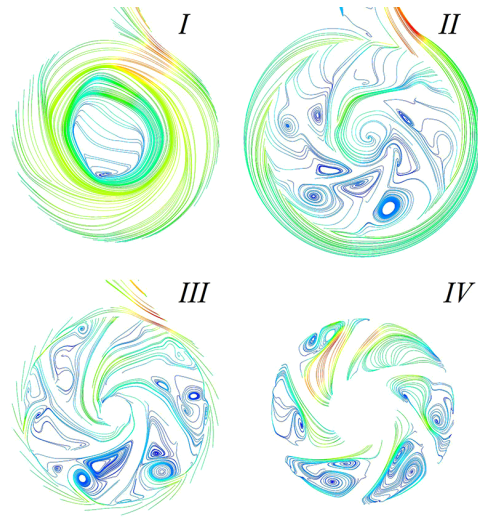


Fig. 11. Distribution of flow lines in a pump of a modified construction $\Delta b_2 = +90$ mm

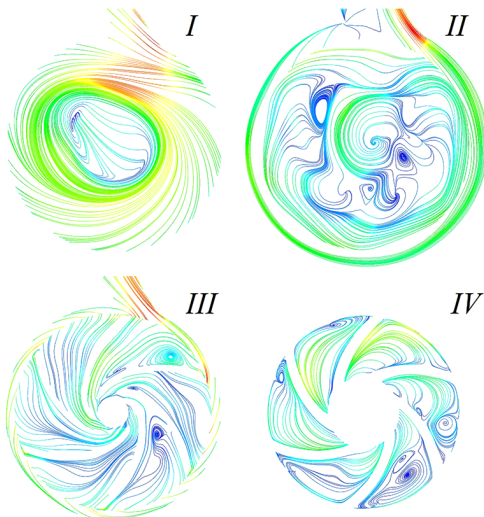


Fig. 10. Distribution of flow lines in a pump of a modified construction $\Delta b_2 = +50$ mm

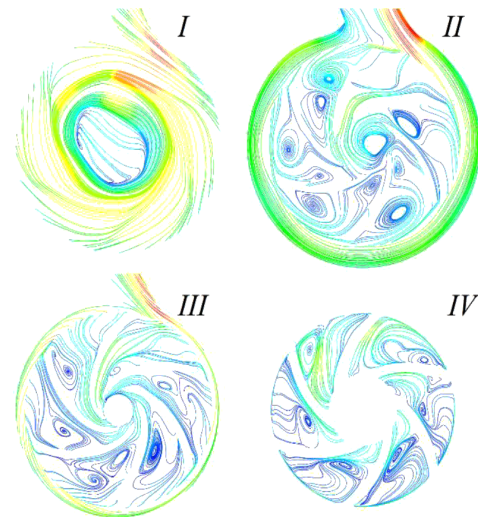


Fig. 12. Distribution of flow lines in a pump of a modified construction $\Delta b_2 = +100$ mm

This is explained by the balance between two main phenomena.

On the one hand, the direct location of the impeller blades in the free chamber enhances the role of the blade operating process, which has a high efficiency and allows centrifugal forces to move the flowing stream directly to the discharge nozzle.

On the other hand, the displacement of the toroidal vortex occurs in the interblade channels of the impeller. In this way, the reverse flow of liquid from the periphery to the axis of the pump actually opposes the flowing stream.

Modified impeller $\Delta b_2 = +90$ mm. Further, in the range of blade expansion $\Delta b_2 = +70$ – $+90$ mm, a rapid increase in the head and efficiency is observed (Fig. 11):

Head: $H_{opt}^{=+90} = 51$ m;

Efficiency: $\eta_{opt}^{=+90} = 0.506$.

Both of the processes mentioned above are still taking place in this mode. Nevertheless, due to the small size of the gap between the edges of the impeller blades and the pump case, the toroidal vortex gradually weakens. This reduces the resistance it exerts on the flowing stream, which is the reason for increasing parameters of the torque-flow pump.

Modified impeller $\Delta b_2 = +100$ mm. With the increasing blade extension $\Delta b_2 = +100$ mm, the pump head continues to increase, but a drop in efficiency is observed (Fig. 12):

Head: $H_{opt}^{=+100} = 55$ m;

Efficiency: $\eta_{opt}^{=+100} = 0.48$.

This is explained by the fact that due to the reduction in the front gap between the stator and the rotor, the toroidal vortex finally collapses. In this way, a torque-flow pump is transformed into a centrifugal pump with a semi-open impeller.

Due to the significant, as for a centrifugal pump, size of the end gap, a reverse flow is formed, caused by the pressure difference on the outer and inner radius of the impeller. This is the reason for the appearance of volumetric losses, which play a major role in reducing the overall efficiency of the pump. Also, due to the difference of velocities in the middle of the interblade channels of the impeller and near its edges, hydraulic energy losses increase.

Conclusions. In this paper, with the use of the ANSYS CFX software complex, the influence of the blade width of the impeller on the integral characteristics of the torque-flow pump was researched in order to reduce hydraulic losses.

The results of the numerical research showed:

1. With increasing the width of the impeller blades, there is increasing of the head and efficiency of the torque-flow pump.

2. One of the reasons for this growth is increasing of the share of the blade operating process and decreasing of the share of the vortex operating process (the maximum theoretic-

cally achievable efficiency of the vortex operating process is 0.5, while that of the bladed is 1.0).

3. While the impeller blades are extended to the free chamber, the liquid under the action of centrifugal forces can be moved directly to the pump discharge nozzle, which increases the role of the blade operating process and reduces the number of fluid rotation cycles in the free pump chamber.

4. With a significant amount of extension, the impeller can interfere with the return of the liquid into the toroidal vortex, which is the reason for the appearance of additional hydraulic losses.

5. While designing torque-flow pumps, it is necessary to choose the amount of the impeller extension to the free chamber in such a way that the total increase in the head and efficiency due to the phenomena described above becomes maximal.

6. The edges of the impeller blades can protrude into the free chamber beyond the position of the center of the toroidal vortex by an insignificant amount, since in this case negative phenomena caused by the deformation of the toroidal vortex and the opposition of centrifugal forces to the return of the liquid are practically not observed.

Acknowledgment. The research was carried out within the NAWA Ulam programme, grant No. BPN/U LM/2022/1/00042.

References.

1. Kovaliov, I., Ratushnyi, A., Dzafarov, T., Mandryka, A., & Ignatiev, A. (2021). Predictive vision of development paths of pump technical systems. *Journal of Physics: Conference Series*, 1741, 012002. <https://doi.org/10.1088/1742-6596/1741/1/012002>.
2. Sotnik, M., Khovansky, S., Grechka, I., Panchenko, V., & Maksimova, M. (2015). Simulation of the thermal state of the premises with the heating system "Heat-insulated floor". *Eastern-European Journal of Enterprise Technologies*, 6(5), 22-27. <https://doi.org/10.15587/1729-4061.2015.56647>.
3. Andrenko, P., Rogovyi, A., Grechka, I., Khovansky, S., & Svyarenko, M. (2021). Characteristics improvement of labyrinth screw pump using design modification in screw. *Journal of Physics: Conference Series*, 1741, 012024. <https://doi.org/10.1088/1742-6596/1741/1/012024>.
4. Kondus, V., & Kotenko, O. (2017). Investigation of the impact of the geometric dimensions of the impeller on the torque flow pump characteristics. *Eastern-European Journal of Enterprise Technologies*, 1/4(88), 25-31. <https://doi.org/10.15587/1729-4061.2017.107112>.
5. Gusak, O., Krishtop, I., German, V., & Baga, V. (2017). Increase of economy of torque flow pump with high specific speed. *IOP Conference Series: Materials Science and Engineering*, 233, 012004. <https://doi.org/10.1088/1757-899X/233/1/012004>.
6. Krishtop, I. (2015). Creating the flowing part of the high energy-efficiency torque flow pump. *Eastern-European Journal of Enterprise Technologies*, 2(74), 31-37.
7. Rogovyi, A., Korohodsky, V., Khovansky, S., Hrechka, I., & Medvediev, Y. (2021). Optimal design of vortex chamber. *Journal of Physics: Conference Series*, 1741, 012018. <https://doi.org/10.1088/1742-6596/1741/1/012018>.
8. Kondus, V., Kalinichenko, P., & Gusak, O. (2018). A method of designing of torque-flow pump impeller with curvilinear blade profile. *Eastern-European Journal of Enterprise Technologies*, 3/8(93), 29-35. <https://doi.org/10.15587/1729-4061.2018.131159>.
9. Ratushnyi, A., Sokhan, A., Kovaliov, I., Mandryka, A., & Ignatiev, O. (2021). Modernization of centrifugal impeller blades. *Journal of Physics: Conference Series*, 1741, 012009. <https://doi.org/10.1088/1742-6596/1741/1/012009>.
10. Gerlach, A., Thamsen, P., Wulff, S., & Jacobsen, C. (2017). Design Parameters of Vortex Pumps: A Meta-Analysis of Experimental Studies. *Energies*, 10(1), 58.
11. Gao, X., Shi, W., Zhang, D., Zhang, Q., & Fang, B. (2014). Optimization design and test of vortex pump based on CFD orthogonal test. *Nongye Jixie Xuebao/Transactions of the Chinese Society for Agricultural Machinery*, 45(5), 101-106.
12. Kondus, V., Puzik, R., German, V., Panchenko, V., & Yakhnenko, S. (2021). Improving the efficiency of the operating process of high specific speed torque-flow pumps by upgrading the flowing part design. *Journal of Physics: Conference Series*, 1741, 012023. <https://doi.org/10.1088/1742-6596/1741/1/012023>.
13. Cervinka, M. (2012). Computational Study of Sludge Pump Design with Vortex Impeller. *Engineering Mechanics*, 87, 191-201.

14. Machalski, A., Skrypacz, J., Szulc, P., & Blonski, D. (2021). Experimental and numerical research on influence of winglets arrangement on vortex pump performance. *Journal of Physics: Conference Series*, (1741). <https://doi.org/10.1088/1742-6596/1741/1/012019>.

15. Kalinichenko, P., Gusak, O., Khovansky, S., & Krutas, Y. (2017). Substantiation and development of the procedure for calculating a hydraulic balancing device under condition of minimal energy losses. *Eastern-European Journal of Enterprise Technologies*, 2(7), 36-41. <https://doi.org/10.15587/1729-4061.2017.97162>.

16. Rogovyi, A., Korohodsky, V., & Medvediev, Y. (2021). Influence of Bingham fluid viscosity on energy performances of a vortex chamber pump. *Energy*, 218, 119432. <https://doi.org/10.1016/j.energy.2020.119432>.

17. Krishtop, I., German, V., Gusak, A., Lugova, S., & Kochevsky, A. (2014). Numerical Approach for Simulation of Fluid Flow in Torque Flow Pumps. In *Applied Mechanics and Materials. Trans Tech Publications, Ltd.*, 630, 43-51. <https://doi.org/10.4028/www.scientific.net/amm.630.43>.

18. Quan, H., Chai, Y., Li, R., & Guo, J. (2019). Numerical simulation and experiment for study on internal flow pattern of vortex pump. *Engineering Computations*, 36, 1579-1596. <https://doi.org/10.1108/EC-09-2018-0420>.

19. Kondus, V., Gusak, O., & Yevtushenko, Y. (2021). Investigation of the operating process of a high-pressure centrifugal pump with taking into account of improvement the process of fluid flowing in its flowing part. *Journal of Physics: Conference Series*, 1741, 012012. <https://doi.org/10.1088/1742-6596/1741/1/012012>.

20. Kulikov, A., Ratushnyi, O., Kovaliov, I., Mandryka, A., & Ignatiev, O. (2021). Numerical study of the centrifugal contra rotating blade system. *Journal of Physics: Conference Series*, 1741, 012008. <https://doi.org/10.1088/1742-6596/1741/1/012008>.

Вплив конструктивних особливостей робочого колеса на комбінований робочий процес вільновихрового насоса

Р. В. Пузік, В. Ю. Кондус*, І. В. Павленко,
С. С. Антоненко

Сумський державний університет, м. Суми, Україна

* Автор-кореспондент e-mail: v.kondus@pgm.sumdu.edu.ua

Мета. Оцінка впливу зміни ширини лопатей робочого колеса на характеристики вільновихрового насоса й пошук оптимальної величини висуву лопаті у вільну камеру насоса. В якості предмета дослідження було обрано вільновихровий насос типу «Туго» СВН 500/32.

Методика. У даній роботі за допомогою програмного комплексу ANSYS CFX було проведено ряд числових експериментів для визначення структури потоку у проточній частині вільновихрового насоса при змінній ширині лопаті робочого колеса. З метою побудови енергетичної й напірної характеристик досліджуваного насоса були визначені його інтегральні параметри.

Результати. Була вивчена та проаналізована структура течії, зокрема тороподібного вихору, у вільновихровому насосі. Була побудована модель течії у вільновихровому насосі базової й модернізованої конструкції. Знайдена залежність зміни параметрів роботи насоса при зміні ширини лопаті робочого колеса в діапазоні від $\Delta_{\min} = -20$ до $\Delta_{\max} = +100$ мм.

Наукова новизна. У роботі було досліджено вплив додаткових гідравлічних втрат, викликаних невідповідністю центру тороподібного вихору та кромок лопатей робочого колеса, на загальні характеристики вільновихрового насоса.

Практична значимість. За допомогою модернізації конструкції робочого колеса було досягнуто значного підвищення параметрів роботи вільновихрового насоса типу «Туго», що дозволяє розширити діапазон його роботи. При цьому не вимагається заміна таких дороговартісних елементів як корпус.

Ключові слова: вільновихровий насос, Ansys CFX, тороподібний вихор, вихровий робочий процес, лопатевий робочий процес

The manuscript was submitted 14.07.22.